LLNL-JRNL-608252

Widely tunable 11 GHz femtosecond fiber laser based on a non-modelocked source

M. Prantil, E. Cormier, J. Dawson, D. Gibson, M. Messerly, C. Barty

December 14, 2012

Optics Letters

Widely tunable 11 GHz femtosecond fiber laser based on a non-modelocked source

Matthew A. Prantil,[1*] Eric Cormier,[2] Jay W. Dawson,[1]
David J. Gibson,[1] Michael J. Messerly,[1] C. P. J. Barty,[1]
[1]*Lawrence Livermore National Laboratory, Livermore, California 94550*
[2]*University of Bordeaux, France*
**Corresponding author: prantil2@llnl.gov*

Received Month X, XXXX; revised Month X, XXXX; accepted Month X, XXXX; posted Month X, XXXX (Doc. ID XXXXX); published Month X, XXXX

An 11 GHz fiber laser built on a modulated CW platform is described and characterized. This compact, vibration-insensitive, fiber based system can be operated at wavelengths compatible with high energy fiber technology, is driven by an RF signal directly, and is tunable over a wide range of drive frequencies. The demonstration system when operated at 1040 nm is capable of 50 ns bursts of 575 micro-pulses produced at a macro-pulse rate of 83 kHz where the macro-pulse and micro-pulse energies are 1.8 μJ and 3.2 nJ respectively. Micro-pulse durations of 850 fs are demonstrated. Extensions to shorter duration are discussed.

OCIS Codes: 060.3510, 140.7090

Very-short-pulse laser sources (in the range of picoseconds to femtoseconds) with high repetition rates (100 MHz to tens of GHz) are needed to drive short-wavelength high-energy photon sources via higher-order nonlinear optical parametric interactions, and as photo-cathode illuminators to create photo-electrons in high frequency particle accelerators. Other applications of these ultrafast pulse laser systems include materials processing, 3-D lithography, high-data-rate laser communication, and remote sensing systems. The system architecture described here is wavelength compatible with high-energy fiber technology, is driven directly by an RF source (and thus sidesteps synchronization issues), and allows for amplification to materials-processing pulse energies. Moreover, the ability to modify electronically the temporal pulse shape, in amplitude and phase [1,2], offers more possibilities.

Unlike traditional methods which rely on mode-locking to produce a train of pulses at the round-trip repetition rate of a laser cavity, we generate a laser pulse train by modulating a continuous-wave (cw) laser with an RF source. Several groups [3-6] have converted cw lasers to sub-ps, high frequency pulse trains; however, these groups have relied on "time-lens" techniques [7] to generate ps-level bandwidths, then used soliton compression in specially optimized fibers to generate further bandwidth while simultaneously compressing the pulse. In the demonstration of this cw-modulation concept reported here, we rely on self-phase modulation (SPM) [8] to generate 3.2 nm of bandwidth and compress the pulse with a grating-pair compressor. To allow high pulse energies at modest average laser power, we temporally chop groups of pulses from the pulse stream; the groups (macro-pulses) occur at mult-kHz rates while the individual pulses (micro-pulses) are at multi-GHz rates. Alternatively, the micro-pulses might be directly amplified to modest energies for a clock-distribution scheme, or driven to micro-joule energies to create tens of kilowatts of power for machining or supercontinuum sources.

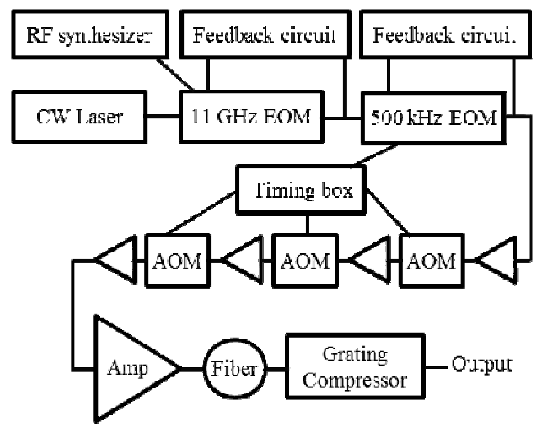

Figure 1 Schematic diagram of the experiment.

The architecture, shown in Figure 1, begins with a cw laser: a New Focus Velocity laser set to provide a 1040 nm beam. The beam is sent through an EOSPACE-brand, Z-cut, 20 GHz, dual drive Mach-Zehnder electro-optic modulator (EOM) monitored by a control circuit (YY Labs, Inc.) to keep the modulator null-biased – that is, biased to block light when the RF drive is off.. This modulator is driven with 20.1 dBm of 5.7 GHz RF power. Because of the null bias, the RF creates an 11.4 GHz laser pulse train with 44 ps pulse length and no cw component as shown in Figure 2; the latter prevents stimulated Brillouin scattering from damaging subsequent fiber amplifiers. A second EOM temporally slices macro-pulses at a 500 kHz rate with 50 ns duration; thus, each macro-pulse contains approximately 575 micro-pulses (Figure 2). Four 6 μm core Yb-doped fiber pre-amplifiers then amplify the pulse train. Crystal

Technology acousto-optic modulators (AOM) are placed between the preamplifiers. The first AOM operates reduces the macro-pulse rate to 500 kHz and the remaining two further reduce the rate to 250 kHz and 83.3 kHz, respectively, while simultaneously removing any inter-pulse amplified spontaneous emission. The macro-pulse shape shown in Figure 3 has some 200 MHz ripple which corresponds to the center frequency of the AOMs. This ripple was minimized to < 10% by aligning the AOMs while monitoring the ripple on a scope. The data in the inset of Figure 3 shows the full modulation that occurs in our system but a 100 ns scan under-samples the data and thus does not display the full modulation depth (this is captured in the inset).

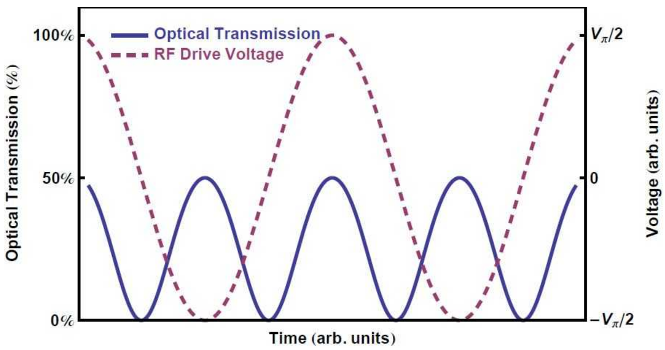

Figure 2 RF drive voltage with null point bias yields a double frequency optical transmission output.

The output of the preamplifier chain is an 83.3 kHz, 20 mW pulse train that is then launched into a large-mode area photonic crystal fiber amplifier (Crystal Fibre PZ-40 with a 29 μm mode field diameter), which boosts the power to 270 mW. The pulse train then passes through an optical isolator and is launched through a lens pair into 300 m of 6 μm polarization maintaining (PM) fiber where self-phase modulation (SPM) increases the pulse-stream's bandwidth to 3.2 nm. We estimate, given the loss from the length of 300 m of fiber, the loss from the splices along its length, and its measured output power of 75 mW, that the input power is 150 mW. With an 83 kHz repetition rate, the energy per macro pulse is 1.8 μJ, which corresponds to a micro-pulse energy of ~3.2 nJ.

To model the expected bandwidth of this system we used a numerical split-step routine to solve the nonlinear Schrödinger equation (NLSE):

$$i\frac{\partial A}{\partial z}=\frac{\beta_2}{2}\frac{\partial^2 A}{\partial t^2}-\frac{2n_2}{\lambda(w_0/2)^2}|A|^2A \qquad (1)$$

where A is the complex pulse envelope, $n_2 = 2.7\times10^{-16}$ cm²/W is the nonlinear index of refraction, $\beta_2 = 0.21$ ps²/m is the quadratic dispersion term for the fiber, $w_0 = 6.6$ μm is the mode field diameter in the fiber, and $\lambda = 1040$ nm is the laser wavelength.

Because our spectral measurement is an aggregation of spectra from > 500 pulses of varying energies, we must account the fact that different pulses may produce different spectra. We first estimated the energies of the micro-pulses by creating a simple envelope matching the measured pulse train (shown in Fig. 3), then normalizing the summed energy of the pulses to match the measured macro-pulse energy. These different energies are run through the NLSE solver.

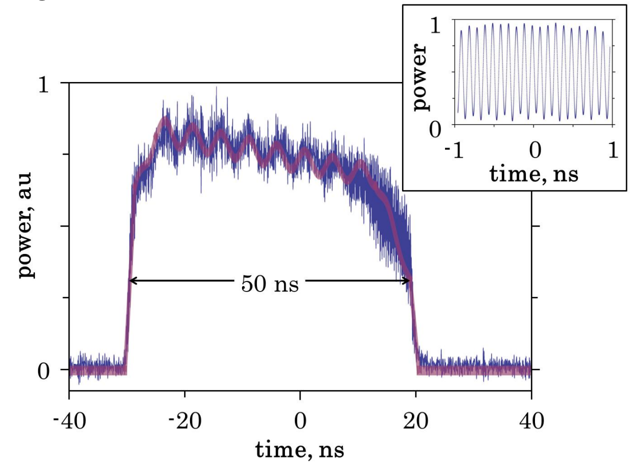

Figure 3 Temporal trace (raw data and smoothed) of the laser macro-pulse recorded using a 12 GHz photodiode, measured after the 300 m length of fiber and before the grating compressor. Inset: Detail of 2 ns window, showing individual pulses.

Figure 4 compares the measured spectrum and simulated spectral envelope after propagating through 300 m of fiber. The pulse shape corresponding to an RF drive voltage of 0.7 V_π is used as an input. High-frequency oscillations on the measured spectrum correspond to the 11.4 GHz repetition rate of the measured pulse train. The agreement between experiment and SPM simulation is exceptionally good as seen below.

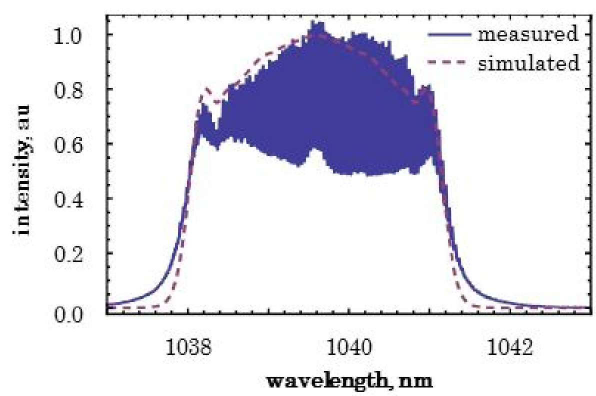

Figure 4 Measured and simulated spectra for a pulse traveling through 300 m fiber.

The high bandwidth pulse train is then passed through a grating pair compressor whose multi-layer dielectric-coated gratings have a groove density of 1740 lines/mm. The angle of incidence on the gratings is 61.8⁰ and the grating slant distance is 260 mm, which was optimized to give the shortest autocorrelation pulsewidth. The output is then characterized in three ways: with an optical spectrum analyzer, a high-speed digital scope coupled to a 12 GHz photodiode, and a home-built autocorrelator in a FROG arrangement. Figure 5 shows the measured autocorrelation after the compressor, which has a full-width, half-maximum (FWHM) of 1.2 ps, implying a pulse width of ~850 fs, in good agreement with the FROG retrieval and close to the transform limit of 700 fs. Roughly 70% of the power lies in the main pulse. The remaining power, which we attribute to high-order dispersive terms in the compressor, lies in the wings and pedestal.

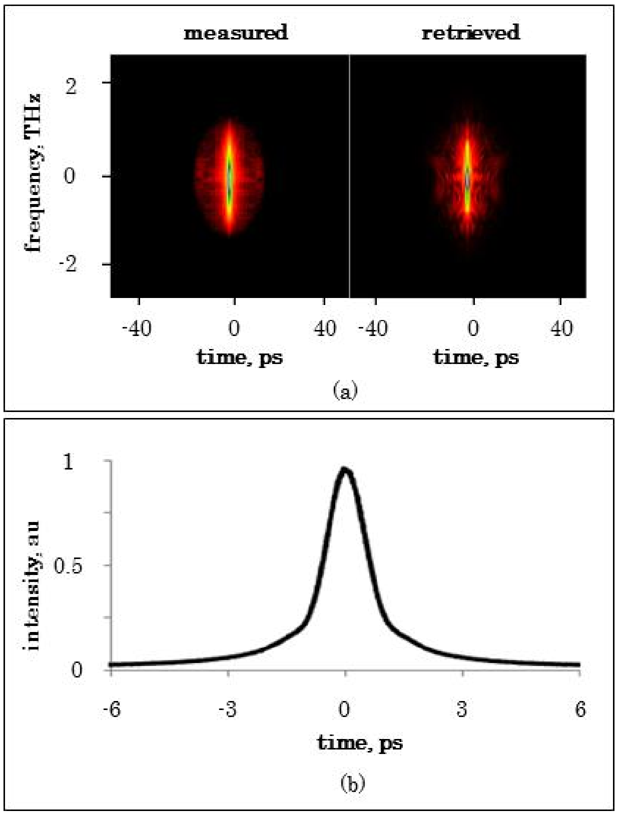

Figure 5 (a) Measured and retrieved FROG traces and (b) autocorrelation of compressed 11.4 GHz pulse train after 300 m of fiber.

The system was tested successfully at RF frequencies between 5 and 20 GHz. The shortest pulses were measured at 11 GHz but all tested frequencies gave pulses compressible to less than 2 ps FWHM, and we expect that the shortness at 11 GHz is due to our alignment optimizations there, and are reinvestigating the other frequencies. The system was also successfully tested with seed wavelengths ranging from 1040 to 1068 nm; 1040 nm was chosen for this Letter because it gave the broadest bandwidth since it falls closest to the gain peak of the Yb-doped amplifiers. Longer wavelengths gave less broadened spectra that were less symmetric than the 1040 nm spectrum due to gain tilt.

The length of PM fiber was initially 200 m; when a 100 m section was added to this, the combined length produced approximately 50 percent more bandwidth, as expected, despite the pulse being more stretched in time due to the additional dispersion of the added fiber. We did not observe more bandwidth, however, because stimulated Raman scattering (SRS) now limited the pulse energy; that is, regardless of fiber length, pulse energies sufficient to generate roughly 4 nm of bandwidth were also energetic enough to generate SRS.

In summary, we have demonstrated a unique system that generates 3.2 nm of compressible bandwidth and produces a pulse train of 1.6 nJ pulses with 11.4 GHz spacing in bursts of 575 pulses each. We plan to further amplify the pulses using an additonal large-mode area photonic crystal fiber amplifier followed by a rod-type amplifier, expecting bursts of μJ level micro-pulses – sufficient to drive a photocathode to feed an X-band accelerator. Shorter pulses with broader compressible bandwidth might be achieved by propagating higher energy pulses through shorter lengths of SPM fiber, or by using multiple SPM stages. The uncorrected phase in the compressed pulses, which leads to a power-robbing pedestal (70% of the power is in main pulse) should be correctible with a fast phase and amplitude corrector, such as the Fastlite Dazzler.

We believe this technique may lead to a new class of oscillators with extremely high repetition rates, that are intrinsically and noiselessly synchronized to their reference clocks, and that provide an extremely stable and robust alternative to conventional mode-locked oscillators.

This work performed under the auspices of the U.S. Department of Energy by Lawrence Livermore National Laboratory under Contract DE-AC52-07NA27344.

References:

1. A.M. Weiner, Optics Communications 284, 3669-3692 (2011).
2. Z. Jiang, C.B. Huang, D.E. Leaird, A.M. Weiner, Nature Photonics 1, 463-467 (2007).
3. C.B. Huang, Z. Jiang, D.E. Leaird, A.M. Weiner, Electronics Letters, 42, 1114-1115 (2006).
4. J. van Howe, J. H. Lee, S. Zhou, F.W. Wise, C. Xu, S. Ramachandran, S. Ghalmi, M.F. Yan, Optics Letters 32(4): 340-342 (2007).
5. I. Morohashi, T. Sakamoto, H. Sotobayashi, T. Kawanishi, I. Hosako, Optics Letters 34, 2297–2299 (2009).
6. B.H. Chapman, A.V. Doronkin, J.M. Stone, J.C. Knight, S.V. Popov, J.R. Taylor, Optics Express 21, 5671-5676. (2013).
7. T. Kobayashi, H. Yao, K. Amano, Y. Fukushima, A. Morimoto, T. Sueta, IEEE J. Quantum. Electron. QE-24, 382–387 (1988).
8. C. V. Shank, R. L. Fork, R. Yen, R.H. Stolen, W.J. Tomlinson, Appl. Phys. Lett. 40, 761–763 (1982).

References:

1. A.M. Weiner, "Ultrafast optical pulse shaping: A tutorial review" Optics Communications 284, 3669-3692 (2011).
2. Z. Jiang, C.B. Huang, D.E. Leaird, A.M. Weiner, "Optical Arbitrary Waveform Processing of More than 100 Spectral Comb Lines," Nature Photonics 1, 463-467 (2007).
3. C.B. Huang, Z. Jiang, D.E. Leaird, A.M. Weiner, "High-Rate Femtosecond Pulse Generation via Line-by-Line Processing of a Phase-Modulated CW Laser Frequency Comb," Electronics Letters, 42, 1114-1115 (2006).
4. J. van Howe, J. H. Lee, S. Zhou, F.W. Wise, C. Xu, S. Ramachandran, S. Ghalmi, M.F. Yan, "Demonstration of soliton self-frequency shift below 1300 nm in higher-order mode, solid silica-based fiber." Optics Letters 32(4): 340-342 (2007).
5. I. Morohashi, T. Sakamoto, H. Sotobayashi, T. Kawanishi, I. Hosako, "Broadband wavelength-tunable ultrashort pulse source using a Mach–Zehnder modulator and dispersion-flattened dispersion-decreasing fiber" Optics Letters 34, 2297–2299 (2009).
6. B.H. Chapman, A.V. Doronkin, J.M. Stone, J.C. Knight, S.V. Popov, J.R. Taylor, "Femtosecond pulses at 20 GHz repetition rate through spectral masking of a phase modulated signal and nonlinear pulse compression" Optics Express 21, 5671-5676. (2013).
7. T. Kobayashi, H. Yao, K. Amano, Y. Fukushima, A. Morimoto, T. Sueta, "Optical Pulse Compression Using High Frequency Electro-Optic Phase Modulation," IEEE J. Quantum. Electron. QE-24, 382–387 (1988).
8. C. V. Shank, R. L. Fork, R. Yen, R.H. Stolen, W.J. Tomlinson, "Compression of femtosecond optical pulses" Appl. Phys. Lett. 40, 761–763 (1982).